ARTICLE

Self-Assembled Nanogaps *via* Seed-Mediated Growth of End-to-End Linked Gold Nanorods

Titoo Jain,[†] Fredrik Westerlund,[†] Erik Johnson,[‡] Kasper Moth-Poulsen,[†] and Thomas Bjørnholm[†,*]

[†]Nano-Science Center and Department of Chemistry, University of Copenhagen, Universitetsparken 5, DK-2100, Copenhagen Ø, Denmark, and [‡]Nano-Science Center and Niels Bohr Institute, University of Copenhagen, Universitetsparken 5, DK-2100 Copenhagen Ø, Denmark, and Department of Quantum Engineering, Nagoya University, Nagoya 4648603, Japan

ABSTRACT Gold nanorods (AuNRs) are of interest for a wide range of applications, ranging from imaging to molecular electronics, and they have been studied extensively for the past decade. An important issue in AuNR applications is the ability to self-assemble the rods in predictable structures on the nanoscale. We here present a new way to end-to-end link AuNRs with a single or few linker molecules. Whereas methods reported in the literature so far rely on modification of the AuNRs after the synthesis, we here dimerize gold nanoparticle seeds with a water-soluble dithiol-functionalized polyethylene glycol linker and expose the linked seeds to growth conditions identical to the synthesis of unlinked AuNRs. Doing so, we obtain a large fraction of end-to-end linked rods, and transmission electron microscopy provides evidence of a 1−2 nm wide gap between the AuNRs. Flow linear dichroism demonstrates that a large fraction of the rods are flexible around the hinging molecule in solution, as expected for a molecularly linked nanogap. By using excess of gold nanoparticles relative to the linking dithiol molecule, this method can provide a high probability that a single molecule is connecting the two rods. In essence, our methods hence demonstrate the fabrication of a nanostructure with a molecule connected to two nanoelectrodes by bottom-up chemical assembly.

KEYWORDS: gold nanorods · self-assembly · linear dichroism · nanogap · molecular electronics

Gold nanorods (AuNRs) have in recent years received increased interest due to ease of synthesis, unique shape-dependent optical properties,[1,2] and potential use in medical[3,4] and electronic applications.[5−7] Shape, size, and aspect ratio of the AuNRs are readily controlled by varying the different parameters in the seed-mediated synthetic route first introduced by Murphy *et al.*[8] AuNRs are typically grown by addition of citrate-stabilized gold nanoparticle seeds to growth solutions containing an amphiphilic molecule.[9] The grown rods can then be subjected to various surface modification schemes, for example, to induce self-assembly.[10−12] There are several reports of self-assembly and arrangement of pregrown AuNRs into different orientations such as side-to-side[13−16] and end-to-end.[14−20] End-to-end assembly has been accomplished using a variety of different protocols: (1) biotin/streptavidin recognition, where addition of a thiol-modified biotin to the AuNRs and subsequent addition of streptavidin leads to the formation of one-dimensional chains of AuNRs;[17] (2) thiol-functionalized oligonucleotides bound to the AuNRs and connected with a DNA linker;[18] (3) polystyrene molecules grafted to the ends of CTAB-coated AuNRs that when exposed to different solvents arrange the AuNRs in rings or chains, all with end-to-end orientation;[19] (4) citrate anions that neutralize the surface charge of the AuNRs, which promotes end-to-end connection.[20] All these end-to-end assemblies have been explained as being due to the fact that the surfactant has stronger affinity for the {100} and {110} crystal planes of the sides of the AuNRs, leaving the {111} facets on the ends more reactive for modifications.[17,21,22] These approaches all rely on modification of the AuNRs after the synthesis by adding the desired linking agent.

Herein, a new strategy for end-to-end self-assembly of AuNRs is reported. Instead of modifying the AuNRs after the growth, we show that end-to-end linked rods can be grown directly from chemically linked seeds. Citrate-stabilized gold nanoparticle seeds are self-assembled using a water-soluble dithiol-functionalized polyethylene glycol (SH-PEG-SH) linker, and then the assembled seeds are exposed to growth conditions[23] in order to grow linked AuNRs (see Figure 1). We investigate the formed nanogap, the assembly process, and the dependence on the SH-PEG-SH concentration by TEM, SEM, and AFM and also introduce flow linear dichroism (flow-LD) as a complementary method to study AuNRs in solution.

A key challenge in the field of molecular electronics is to contact a single molecule

*Address correspondence to tb@nano.ku.dk.

Received for review January 22, 2009 and accepted March 03, 2009.

Published online March 13, 2009. 10.1021/nn900066w CCC: $40.75

to two or more metal electrodes. Typically macroscopic electrodes fabricated by advanced top-down lithographic techniques are used to contact the molecule of interest.[24,25] Examples of assembling probing electrodes around single molecules *via* bottom-up self-assembly are very few.[26−28] The use of 500 nm long gold nanorods as the bridge between a single molecule on the molecular scale and the straightforwardly accessible micron scale is therefore very tempting. As a consequence of the strategy presented here, it will be possible to synthesize pairs of rods with—to a high extent—only one molecule as linking moiety.

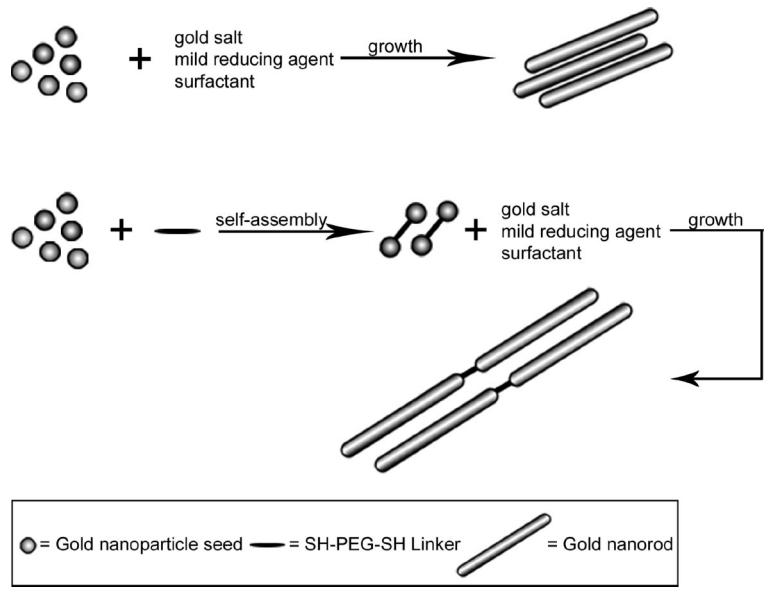

Figure 1. Fabrication scheme of gold nanorods. Top scheme: Seed-mediated growth route for synthesis of AuNRs, which are typically postmodified with desired linkers to create one-dimensional end-to-end linked linear chains as described in the text. Bottom scheme: Our new approach for direct synthesis and growth of end-to-end linked AuNRs using gold nanoparticle seeds that are linked with a SH-PEG-SH linker before addition to the growth solution.

RESULTS AND DISCUSSION

Gold nanorods (AuNRs) are here prepared by a three-step seed-mediated synthesis according to the protocol by Jana *et al.*:[23] Citrate-stabilized nanoparticle seeds are synthesized by reduction of a gold salt with a strong reducing agent and then added to growth solutions containing gold salt, a mild reducing agent, and a surfactant. In this study, we grow end-to-end linked AuNRs by assembling the seed particles before growth, using a water-soluble polyethylene glycol dithiol (SH-PEG-SH) linker. In order to obtain optimal growth conditions for linked AuNR dimers, the seed particles were assembled using varying SH-PEG-SH concentrations (1.67 μM to 0.33 mM). The seed particle concentration is estimated to be approximately 80 nM. Addition of SH-PEG-SH to the citrate-stabilized seeds leads to a small red shift of the surface plasmon resonance band in the absorption spectrum (at around 520 nm), a shift that increases with increasing SH-PEG-SH concentration (see Supporting Information, Figure S1). The shift is accompanied by a broadening of the absorption peak and an increased light scattering. This is in agreement with what is expected for gold nanoparticles in close proximity to each other.[29] Seed particles linked with different amounts of SH-PEG-SH were then subjected to the AuNR growth protocol (for further details see Materials and Methods). At low SH-PEG-SH concentration in the seeding solution (<8.33 μM), the grown rods are only linked to a very small extent (see Supporting Information, Figure S2A). At high concentrations of SH-PEG-SH (>83.3 μM), a majority of the grown AuNRs are linked, but the yield of rods is low and a large amount of spherical particles can be seen (Figure S2D). The spherical particles are typically found as dimers, trimers, or larger assemblies, due to the SH-PEG-SH linker. Apparently, higher concentrations of SH-PEG-SH inhibit growth of AuNRs. A plausible explanation for this is that a too high surface concentration of SH-PEG-SH hinders the binding of CTAB to the seeds and hence AuNRs cannot be grown. The optimal SH-PEG-SH concentration in the seed solution is thus found to be in the range of 16.7−41.7 μM, where a high fraction of the seeds are grown into AuNRs and a large number of the grown rods are linked (Figure S2B and S2C in Supporting Information). All results discussed in the following are on AuNRs grown from gold nanoparticle seeds containing 16.7 μM of SH-PEG-SH. To confirm that the linked rods are not formed after the growth is completed, due to free SH-PEG-SH in solution, a series of control experiments were conducted. An increasing amount of SH-PEG-SH was added to unlinked AuNRs, that is, rods grown from seeds without SH-PEG-SH linker (see Supporting Information, Figure S3). This results in the formation of large random aggregates of AuNRs at moderate concentrations of SH-PEG-SH (16.7 and 83.3 μM) with no obvious end-to-end linking. Even at 0.33 mM SH-PEG-SH, no end-to-end linking is observed. This manifests that our linked rods are grown from chemically linked gold nanoparticle seeds and not linked due to excess SH-PEG-SH in the final growth solution.

Figure 2 compares AuNRs grown from unlinked seed particles (*i.e.*, no SH-PEG-SH linker) and AuNRs grown from gold nanoparticle seeds containing 16.7 μM of SH-PEG-SH. Unlinked rods preferentially lie in a side-to-side fashion (Figure 2A,B) on the TEM grid, which is attributed to a more energetically favorable interaction between the lipophillic parts of the stabilizing surfactant bilayer covering the AuNRs.[20,23] In addition to this side-to-side arrangement, a large amount of end-to-end orientations are observed for the AuNRs grown from chemically linked seed particles (Figure 2C−F). From TEM images, we observe that the dimensions of the linked and unlinked AuNRs are similar with a length of approximately 500 nm and a width of 25

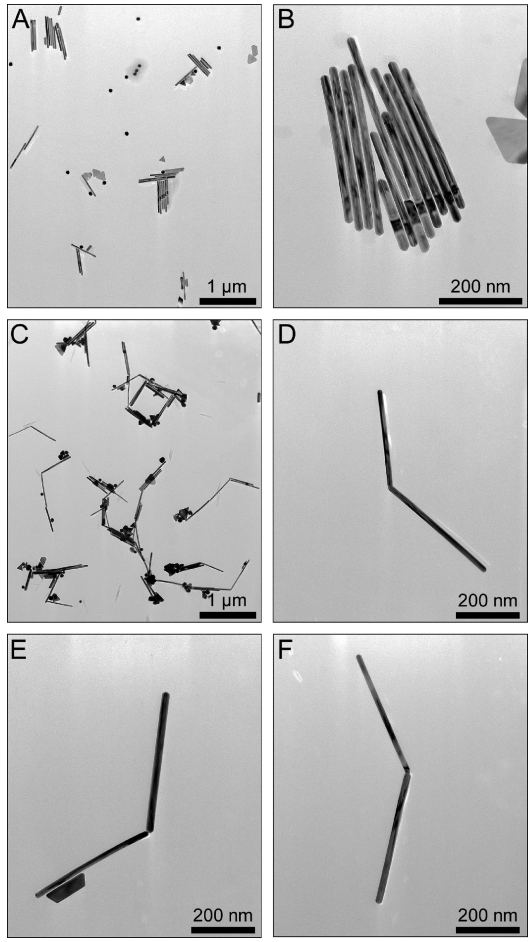

Figure 2. TEM images comparing linked and unlinked rods. Representative TEM images of unlinked AuNRs grown from normal seed particles, that is, no SH-PEG-SH (A,B) and of linked AuNRs synthesized from chemically linked seeds particles, 16.7 μM SH-PEG-SH (C−F).

nm and, hence, an aspect ratio of approximately 20 (data not shown). This is in agreement with what is expected from the growth protocol used.[30] In addition to TEM imaging, the AuNRs were investigated with SEM and AFM (see Supporting Information, Figures S4 and S5, respectively), yielding similar results.

Counting the rods in several TEM images reveals that 55% of the AuNRs grown from chemically linked seed particles (16.7 μM SH-PEG-SH) are end-to-end linked, while only 9% are end-to-end linked for AuNRs grown from unlinked seeds (Figure 3A). The histogram also reveals that for the linked rods the fraction of connections where more than two rods are sharing the same junction is less than 10%. End-to-side linked rods are rarely seen, suggesting that the dithiols move to the ends of the rods where the CTAB is less densely packed as the rods grow. The angle distribution of end-to-end linked AuNRs (Figure 3B) shows a mean value of 125 ± 30°, and very few rods with an angle of less than 90° are observed. This is similar to the end-to-end linked AuNRs investigated by Kawamura *et al.*[20] They explain the angle as being due to the fact that the positively charged CTAB bilayers on the rods repel each other, but it could in our case also be explained as an effect of that small angles between the linked AuNRs will result in too much strain on the SH-PEG-SH linkers.

The crystallography and packing microstructure of the nanorods was determined from fast Fourier transform (FFT) analysis of HRTEM micrographs (Figure 4). Both the linked and unlinked rods are typically multicrystalline and composed of five parallel segments with {111} end faces and {100} side faces organized in a multiply twinned structure similar to that described by Johnson *et al.* for unlinked rods.[31]

Figure 4A shows a high-resolution TEM image where a nanogap with a size of 1−2 nm between two rods is clearly seen, while Figure 4B shows two linked rods that are fused together, both structures being frequently present in the samples investigated. In order to see whether the electron beam could induce fusing of the linked rods, the area in Figure 4A was exposed to a high intensity electron beam for 5 min without any signifi-

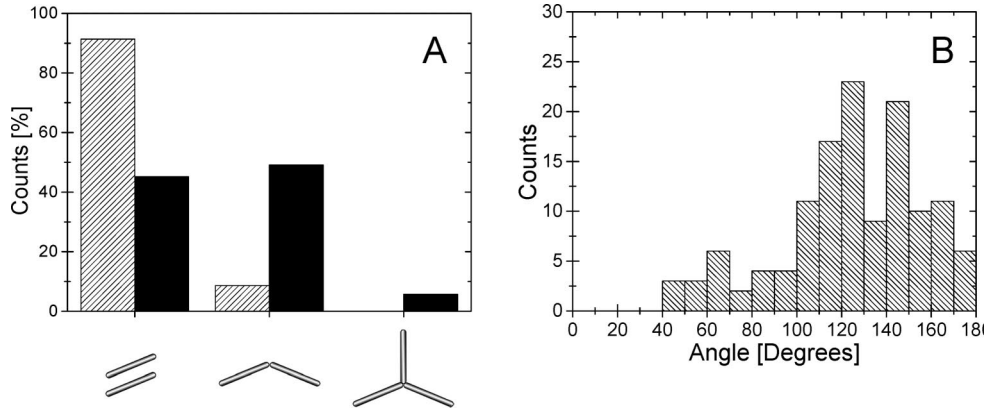

Figure 3. Histogram of rod−rod connections and rod−rod angles. (A) Fraction of unlinked AuNRs (left), AuNRs in dimers or chains (middle), and AuNRs sharing a junction with more than one other rod (right) for AuNRs grown from unlinked seed particles (gray) and AuNRs synthesized from chemically linked seed particles, 16.7 μM SH-PEG-SH (black). The data are obtained from counting approximately 600 AuNRs at different positions from at least four different AuNR batches for each type of rod. (B) Angle distribution between two end-to-end linked rods grown from seeds linked with 16.7 μM of SH-PEG-SH. The mean angle is 125°, and the standard deviation is 30°.

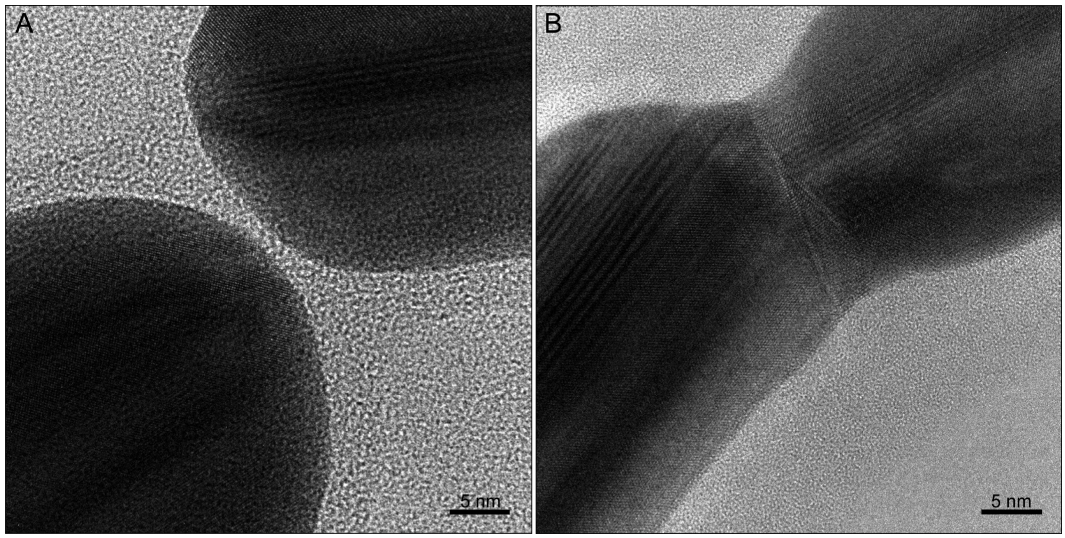

Figure 4. High-resolution TEM images of the linkage between two nanorods: (A) 1−2 nm nanogap between two rods; (B) fused nanogap.

cant changes in the gap region (not shown). The size of the nanogaps seen throughout the samples is typically 1−2 nm and is thus perfectly suited for single molecule electronics. To use the nanogap for measurements on electronically interesting molecules, it can be exposed to a solution of the molecule of interest and then one or a few molecules will be present in the gap.[32,33] The other possibility is to start with an electronically interesting molecule that is water-soluble and use that as a linker to assemble the seeds instead of the SH-PEG-SH. At a 16.7 μM SH-PEG-SH concentration, it is expected that more than one linker molecule is bound to each seed particle and hence that the gap most likely consists of a few linker molecules. We here focused on optimizing the yield of linked rods, and the linker concentration is therefore higher than the concentration of gold nanoparticle seeds. Nanogaps with only one linker molecule in the gap can be realized by the addition of a smaller amount of SH-PEG-SH to the seeds, similar to the method applied by Dadosh and coworkers for monofunctionalized nanoparticles.[26,34]

In addition to the nanogaps, we also observe fused nanorods (Figure 4B). Fused rods have previously been observed by Kawamura *et al.* when they end-to-end linked AuNRs by adding citrate anions after the growth.[20] They reasoned that the fusing was caused by a dilution of CTAB at the ends of the rods due to the previously discussed preferential binding of CTAB to the {100} or {110} facets on the side of the AuNRs. The electrostatic repulsion between the positively charged head groups decreases when CTAB is primarily removed from the ends, and AuNRs that are oriented end-to-end in close proximity may fuse as gold nanoparticles are known to sinter at temperatures as low as 100−200 °C.[35,36] In addition to this explanation, we speculate that the fusing occurs when solvent evaporates from the solid substrate.

An important question arising in the TEM study is whether the fusing of the AuNRs is an effect of the preparation of the samples or if the rods are fused already in solution. To investigate the nature of the linking of the gold nanorods in solution, we decided to use linear dichroism (LD), that is, the difference in absorption parallel and perpendicular to an orientation axis ($LD(\lambda) = A_{\parallel}(\lambda) - A_{\perp}(\lambda)$). Nanoscale objects with large aspect ratios can be aligned easily in a viscous flow, for example in a Couette cell (Figure 5A), and hence the LD spectrum can be obtained by measuring the absorption parallel and perpendicular to the orientation axis. This technique has been extensively used to study DNA and ligands that bind to DNA.[37] The DNA bases are oriented at 90° relative to the DNA helix axis (and hence the orientation axis), and therefore, DNA will have a large negative LD signal at 260 nm, where the bases absorb. Knowing this, it is possible to investigate ligands[38] and proteins[39] that bind to DNA and determine their orientation relative to the DNA axis. Flow-LD has also been used to study, for example, brain microtubules[40] and ligands binding to lipid membranes.[41]

Figure 5B shows LD spectra for unlinked AuNRs and AuNRs grown from a solution with seeds containing 16.7 μM of SH-PEG-SH. There is a large peak in both spectra centered at approximately 515 nm corresponding to the transversal surface plasmon resonance (SPR) peak seen in UV−vis absorption (top panel). As expected, the peak is negative since it is due to a transition perpendicular to the orientation direction. The longitudinal SPR transition has its maximum absorption in the near-IR and can therefore not be investigated in this experimental setup. It is evident that the linked rods have a much more negative LD signal from their transversal SPR band than the unlinked rods. This can be explained from the assumption that the linked AuNRs are larger objects with a larger aspect ratio, and that

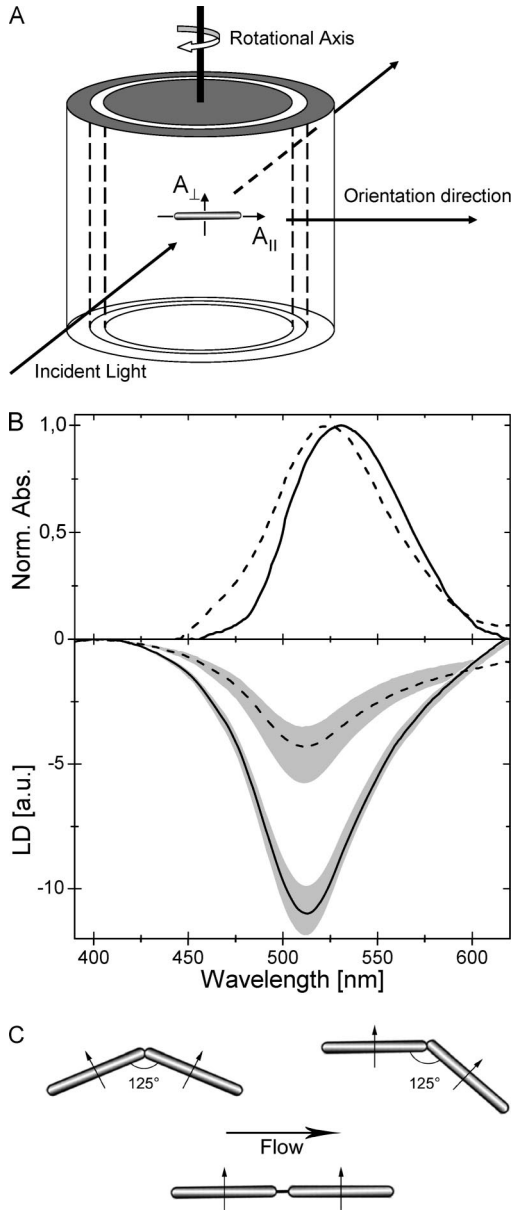

Figure 5. Flow aligned linear dicroism. (A) Schematic showing the principle of flow-LD in a Couette cell. The absorption directions parallel ($A_\parallel$) and perpendicular ($A_\perp$) to the flow, and hence the AuNR long axis, are pointed out. (B) UV−vis absorption (top) and flow-LD (bottom) spectra of normal AuNRs (dashed line) and AuNRs grown from nanoparticle seeds linked with 16.7 μM SH-PEG-SH (solid line). The LD spectra are the average of 4−5 spectra from 2−3 different batches of rods. All spectra within each sample series fall in the shaded areas. The LD spectra have been corrected for the isotropic absorption intensity and normalized to 0 at 400 nm to allow comparison. The UV−vis spectra have been corrected for scattered light. (C) Schematic of the direction of the two transversal SPR transitions (arrows) of linked (fused) AuNR dimers (angle between AuNRs = 125°) relative to the orientation axis in a viscous flow (top). Two extreme cases are shown, and they both have a significant component of the SPR transition along the orientation axis, a component that has a positive LD signal. Two nonfused AuNRs linked with a linker (bottom), on the other hand, will both align with the flow and the transversal band will thus be aligned perpendicular to the flow for both rods leading to only a negative LD component.

they therefore align better with the flow than unlinked AuNRs. A better orientation will lead to a larger difference in the absorption in the two polarization directions and hence a more negative LD signal. An important aspect with flow-LD is that only objects that are oriented in the flow will be visible in LD since all other objects will have a random distribution of their transition moments and, therefore, no LD signal. In our study, this means that we are only probing the AuNRs and not the spherical particles that are also formed during the preparation of the rods. Flow-LD can thus be used to "filtrate" the sample to only detect signal from the AuNRs.

The average angle between the AuNRs, determined from TEM studies, is 125 ± 30° (Figure 3), and if these angles were present in fused rods already existing in solution, both of the rods would not be able to simultaneously align perfectly with the flow. As sketched in Figure 5C, two AuNRs that are fused will have a significant component of their total transversal absorption parallel with the flow, which should lead to a lowering of the LD signal compared to two unlinked rods. The LD signal for the linked AuNRs is more than twice the signal for unlinked AuNRs. Assuming that the yield of rods is not higher for linked rods than for unlinked rods (as seen from several TEM images), the LD results suggest that both rods in the dimers are well-oriented with the flow. Thus the LD measurements indicate that the linked AuNRs are not fused in solution. It should be noted that the LD study cannot exclude the less likely case that some of the rods are fused so weakly that the shear flow changes the angle between the two. To be able to draw quantitative conclusions about the degree of alignment, a thorough LD study of gold rods of different aspect ratios is required (work in progress).

CONCLUSION

In summary, we have introduced a new approach to the synthesis of end-to-end linked gold nanorods (AuNRs). While previous schemes for end-to-end linking of AuNRs all involve modification of the AuNR after the growth is completed, it has here been shown that end-to-end linked rods can be formed by assembling the seeds before the rod synthesis. Adding a water-soluble dithiol PEG molecule (MW = 3400) to citrate-stabilized gold nanoparticle seeds leads to the formation of linked seeds that can subsequently be used to form nanorods *via* a standard growth procedure. We show that we can form a nanogap of 1−2 nm between the rods, a size that is perfectly suited for single molecule electronics. In this report, we focused on optimizing the yield of linked rods, and the applied concentration of SH-PEG-SH is therefore much higher than the concentration of seeds. By using excess of gold nanoparticles relative to the linking dithiol molecule, this method can provide access to a single molecule

connecting two rods. In essence, our method hence demonstrates a possible way to fabricate a nanostructure with a single molecule connected between two nanoelectrodes by bottom-up chemical assembly.

A fraction of the formed AuNRs dimers appears fused in TEM, and we speculate that the fusing is partly due to evaporation of the solvent on the solid substrate. Flow-LD was introduced as a suitable tool to study AuNRs in solution. By aligning the AuNRs in a flow, the absorption parallel and perpendicular to the long axis of the AuNR can be measured. It was observed that the linked AuNRs align much better with the flow, and we argue that it is because the rods are to a large extent not fused in solution.

MATERIALS AND METHODS

Materials. Cetyltrimethylammonium bromide (CTAB, 99%), sodium tetrahydridoborate ($NaBH_4$, 99%), and hydrogen tetrachloroaurate(III) trihydrate ($HAuCl_4$, 99.9%) were obtained from Aldrich Chemicals. Ascorbic acid and trisodium citrate (>99%) were obtained from Merck. Dithiol-functionalized polyethylene glycol, $SHCH_2CH_2O(CH_2CH_2O)_nCH_2CH_2SH$, $n \approx 65$ (SH-PEG-SH, MW = 3400), was obtained from Laysan Bio. All reagents were used as received, and all glassware was thoroughly cleaned with a solution of sulfuric acid and potassium dichromate before use. Water was purified using a Millipore-MilliQ setup for ultrapure water (18.2 MΩ).

Synthesis and Assembly of Gold Seeds. The synthesis of citrate-stabilized gold seeds was carried out as described elsewhere.[23] Briefly, gold seeds were prepared by adding 0.5 mL of 0.01 M aqueous $HAuCl_4$ and 0.5 mL of 0.01 M aqueous sodium citrate to 18.4 mL of MilliQ water under magnetic stirring. Then 0.6 mL of freshly prepared ice-cold 0.1 M $NaBH_4$ was added, and the solution changed from colorless to red/orange, indicating seed particle formation. Stirring was stopped, and the seeds were left undisturbed for 2 h; the synthesis was performed under nitrogen atmosphere. For assembly of gold seeds, SH-PEG-SH solutions of different concentrations were prepared in degassed water and added to the gold seeds to leave final SH-PEG-SH concentrations in the seed solutions ranging from 1.67 μM to 0.33 mM. The addition of SH-PEG-SH to the seeds induced a small color change from red/orange to light red/purple, indicating assembly of the particles. The solution was stirred briefly by vortexing and left undisturbed for 1 h.

Growth of End-to-End Linked Gold Nanorods. The growth of AuNRs follows the procedure described elsewhere.[30] In brief, three centrifuge tubes were labeled A, B, and C. Each consisted of 9 mL of 0.1 M CTAB, 0.25 mL of 0.01 M $HAuCl_4$, and 50 μL of 0.1 M ascorbic acid. One milliliter of the linked seeds was added to the growth solution in tube A, which was inverted 10 times to mix and left for 30 s. One milliliter was transferred from tube A to tube B, which was inverted 10 times to mix and left for 60 s. One milliliter was transferred from tube B to the tube containing growth solution C, which was inverted 10 times to mix and left undisturbed for 48 h at 27 °C. The rods settled at the bottom, and the top solution, consisting mainly of spherical particles, was discarded. The rods were further purified by several rounds of centrifugation. Note that, for synthesis of unlinked nanorods, 1 mL of seed particles with no SH-PEG-SH linker was added to tube A instead, and then an identical growth protocol was used.

TEM. Conventional transmission electron micrographs (TEM) were obtained on a Philips CM20 instrument operated at 200 kV, while high-resolution micrographs were obtained with a JEOL JEM 2010F HRTEM (200 kV field emission gun). For TEM imaging, a droplet of sonicated gold rods was cast on Formvar copper grids and left to evaporate.

Flow-LD and UV−Vis Measurements. Linear dichroism is defined as the difference in absorbance of linearly polarized light parallel and perpendicular to a macroscopic orientation axis (here the flow direction): $LD(\lambda) = A_{\parallel}(\lambda) - A_{\perp}(\lambda)$. Samples with unlinked or linked gold nanorods were oriented in a Couette flow cell with an outer rotating cylinder at a shear gradient of 3000 s^{-1}. LD spectra were measured on a Jasco J-720 CD spectropolarimeter equipped with an Oxley prism to obtain linearly polarized light. All spectra were baseline-corrected by subtracting the spectrum recorded for the non-oriented sample. All LD spectra were corrected for the isotropic absorption. The isotropic UV−vis spectra were recorded on a Jasco V-530 and corrected for scattered light.

Acknowledgment. The work was supported by the European Community Seventh Framework Program (FP7/2007−2013) under the grant agreement no. 213609 "SINGLE" and the Danish Research Councils. F.W. acknowledges the Knut and Alice Wallenberg foundation for funding. E.J. acknowledges a fellowship from The Greater Nagoya Invitation Program for International Research Scientists in Environmental Science Field operated by Chubu Science and Technology Center Foundation. We acknowledge Professor Bengt Nordén for kindly letting us use the LD instrument at the Department of Chemical and Biological Engineering/Physical Chemistry, Chalmers University of Technology.

Supporting Information Available: UV−vis measurements of linked and unlinked seed particles, TEM images of AuNRs reacted with SH-PEG-SH linker post synthesis, AuNRs grown at different SH-PEG-SH concentration, as well as SEM and AFM images of linked and unlinked AuNRs. This material is available free of charge *via* the Internet at http://pubs.acs.org.

REFERENCES AND NOTES

1. El-Sayed, M. A. Some Interesting Properties of Metals Confined in Time and Nanometer Space of Different Shapes. *Acc. Chem. Res.* **2001**, *34*, 257–264.
2. Perez-Juste, J.; Pastoriza-Santos, I.; Liz-Marzan, L. M.; Mulvaney, P. Gold Nanorods: Synthesis, Characterization and Applications. *Coord. Chem. Rev.* **2005**, *249*, 1870–1901.
3. Wang, H.; Huff, T. B.; Zweifel, D. A.; He, W.; Low, P. S.; Wei, A.; Cheng, J.-X. *In Vitro* and *In Vivo* Two-Photon Luminescence Imaging of Single Gold Nanorods. *Proc. Natl. Acad. Sci. U.S.A.* **2005**, *102*, 15752–15756.
4. Huang, X.; Jain, P. K.; El-Sayed, I. H.; El-Sayed, M. A. Plasmonic Photothermal Therapy (PPTT) Using Gold Nanoparticles. *Lasers Med. Sci.* **2008**, *23*, 217–228.
5. Smith, P. A.; Nordquist, C. D.; Jackson, T. N.; Mayer, T. S.; Martin, B. R.; Mbindyo, J.; Mallouk, T. E. Electric-Field Assisted Assembly and Alignment of Metallic Nanowires. *Appl. Phys. Lett.* **2000**, *77*, 1399–1401.
6. Mbindyo, J. K. N.; Mallouk, T. E.; Mattzela, J. B.; Kratochvilova, I.; Razavi, B.; Jackson, T. N.; Mayer, T. S. Template Synthesis of Metal Nanowires Containing Monolayer Molecular Junctions. *J. Am. Chem. Soc.* **2002**, *124*, 4020–4026.
7. Cai, L. T.; Skulason, H.; Kushmerick, J. G.; Pollack, S. K.; Naciri, J.; Shashidhar, R.; Allara, D. L.; Mallouk, T. E.; Mayer, T. S. Nanowire-Based Molecular Monolayer Junctions: Synthesis, Assembly, and Electrical Characterization. *J. Phys. Chem. B* **2004**, *108*, 2827–2832.
8. Jana, N. R.; Gearheart, L.; Murphy, C. J. Seed-Mediated Growth Approach for Shape-Controlled Synthesis of Spheroidal and Rod-Like Gold Nanoparticles Using a Surfactant Template. *Adv. Mater.* **2001**, *13*, 1389–1393.
9. Grzelczak, M.; Perez-Juste, J.; Mulvaney, P.; Liz-Marzan, L. M. Shape Control in Gold Nanoparticle Synthesis. *Chem. Soc. Rev.* **2008**, *37*, 1783–1791.
10. Dai, Q.; Coutts, J.; Zou, J.; Huo, Q. Surface Modification of Gold Nanorods through a Place Exchange Reaction Inside an Ionic Exchange Resin. *Chem. Commun.* **2008**, 2858–2860.

11. Gole, A.; Murphy, C. J. Azide-Derivatized Gold Nanorods: Functional Materials for "Click" Chemistry. *Langmuir* **2008**, *24*, 266–272.
12. Gole, A.; Stone, J. W.; Gemmill, W. R.; zur Loye, H.-C.; Murphy, C. J. Iron Oxide Coated Gold Nanorods: Synthesis, Characterization, and Magnetic Manipulation. *Langmuir* **2008**, *24*, 6232–6237.
13. Gole, A.; Murphy, C. J. Biotin-Streptavidin-Induced Aggregation of Gold Nanorods: Tuning Rod−Rod Orientation. *Langmuir* **2005**, *21*, 10756–10762.
14. Murphy, C. J.; Sau, T. K.; Gole, A. M.; Orendorff, C. J.; Gao, J.; Gou, L.; Hunyadi, S. E.; Li, T. Anisotropic Metal Nanoparticles: Synthesis, Assembly, and Optical Applications. *J. Phys. Chem. B* **2005**, *109*, 13857–13870.
15. Murphy, C. J.; Gole, A. M.; Hunyadi, S. E.; Orendorff, C. J. One-Dimensional Colloidal Gold and Silver Nanostructures. *Inorg. Chem.* **2006**, *45*, 7544–7554.
16. Westerlund, F.; Bjørnholm, T. Directed Assembly of Gold Nanoparticles. *Curr. Opin. Colloid Interface Sci.* **2009**, *14*, 126–134.
17. Caswell, K. K.; Wilson, J. N.; Bunz, U. H. F.; Murphy, C. J. Preferential End-to-End Assembly of Gold Nanorods by Biotin-Streptavidin Connectors. *J. Am. Chem. Soc.* **2003**, *125*, 13914–13915.
18. Pan, B.; Ao, L.; Gao, F.; Tian, H.; He, R.; Cui, D. End-to-End Self-Assembly and Colorimetric Characterization of Gold Nanorods and Nanospheres *via* Oligonucleotide Hybridization. *Nanotechnol.* **2005**, *16*, 1776–1780.
19. Nie, Z.; Fava, D.; Kumacheva, E.; Zou, S.; Walker Gilbert, C.; Rubinstein, M. Self-Assembly of Metal-Polymer Analogues of Amphiphilic Triblock Copolymers. *Nat. Mater.* **2007**, *6*, 609–614.
20. Kawamura, G.; Yang, Y.; Nogami, M. End-to-End Assembly of CTAB-Stabilized Gold Nanorods by Citrate Anions. *J. Phys. Chem. C* **2008**, *112*, 10632–10636.
21. Thomas, K. G.; Barazzouk, S.; Ipe, B. I.; Joseph, S. T. S.; Kamat, P. V. Uniaxial Plasmon Coupling through Longitudinal Self-Assembly of Gold Nanorods. *J. Phys. Chem. B* **2004**, *108*, 13066–13068.
22. Chang, J.-Y.; Wu, H.; Chen, H.; Ling, Y.-C.; Tan, W. Oriented Assembly of Au Nanorods Using Biorecognition System. *Chem. Commun.* **2005**, 1092–1094.
23. Jana, N. R.; Gearheart, L.; Murphy, C. J. Wet Chemical Synthesis of High Aspect Ratio Cylindrical Gold Nanorods. *J. Phys. Chem. B* **2001**, *105*, 4065–4067.
24. Joachim, C.; Gimzewski, J. K.; Schlittler, R. R.; Chavy, C. Electronic Transparence of a Single C60 Molecule. *Phys. Rev. Lett.* **1995**, *74*, 2102–2105.
25. Bumm, L. A.; Arnold, J. J.; Cygan, M. T.; Dunbar, T. D.; Burgin, T. P.; Jones, L., II; Allara, D. L.; Tour, J. M.; Weiss, P. S. Are Single Molecular Wires Conducting? *Science* **1996**, *271*, 1705–1707.
26. Dadosh, T.; Gordin, Y.; Krahne, R.; Khivrich, I.; Mahalu, D.; Frydman, V.; Sperling, J.; Yacoby, A.; Bar-Joseph, I. Measurement of the Conductance of Single Conjugated Molecules. *Nature* **2005**, *436*, 677–680.
27. Martin, C. A.; Ding, D.; Sørensen, J. K.; Bjørnholm, T.; van Ruitenbeek, J. M.; van der Zant, H. S. J. Fullerene-Based Anchoring Groups for Molecular Electronics. *J. Am. Chem. Soc.* **2008**, *130* (40), 13198–13199.
28. Ulgut, B.; Abruna, H. D. Electron Transfer through Molecules and Assemblies at Electrode Surfaces. *Chem. Rev.* **2008**, *108*, 2721–2736.
29. Daniel, M.-C.; Astruc, D. Gold Nanoparticles: Assembly, Supramolecular Chemistry, Quantum-Size-Related Properties, and Applications toward Biology, Catalysis, and Nanotechnology. *Chem. Rev.* **2004**, *104*, 293–346.
30. Gao, J.; Bender, C. M.; Murphy, C. J. Dependence of the Gold Nanorod Aspect Ratio on the Nature of the Directing Surfactant in Aqueous Solution. *Langmuir* **2003**, *19*, 9065–9070.
31. Johnson, C. J.; Dujardin, E.; Davis, S. A.; Murphy, C. J.; Mann, S. Growth and Form of Gold Nanorods Prepared by Seed-Mediated, Surfactant-Directed Synthesis. *J. Mater. Chem.* **2002**, *12*, 1765–1770.
32. Hassenkam, T.; Moth-Poulsen, K.; Stuhr-Hansen, N.; Nørgaard, K.; Kabir, M. S.; Bjørnholm, T. Self-Assembly and Conductive Properties of Molecularly Linked Gold Nanowires. *Nano Lett.* **2004**, *4*, 19–22.
33. van der Zant, H. S. J.; Osorio, E. A.; Poot, M.; O'Neill, K. Electromigrated Molecular Junctions. *Phys. Status Solidi B* **2006**, *243*, 3408–3412.
34. Brousseau, L. C., III; Novak, J. P.; Marinakos, S. M.; Feldheim, D. L. Assembly of Phenylacetylene-Bridged Gold Nanocluster Dimers and Trimers. *Adv. Mater.* **1999**, *11*, 447–449.
35. Buffat, P. A. Lowering of the Melting Temperature of Small Gold Crystals Between 150 Å and 25 Å Diameter. *Thin Solid Films* **1976**, *32*, 283–286.
36. Hassenkam, T.; Nørgaard, K.; Iversen, L.; Kiely, C. J.; Brust, M.; Bjørnholm, T. Fabrication of 2D Gold Nanowires by Self-Assembly of Gold Nanoparticles on Water Surfaces in the Presence of Surfactants. *Adv. Mater.* **2002**, *14*, 1126–1130.
37. Nordén, B.; Kubista, M.; Kurucsev, T. Linear Dichroism Spectroscopy of Nucleic Acids. *Q. Rev. Biophys.* **1992**, *25*, 51–170.
38. Wilhelmsson, L. M.; Westerlund, F.; Lincoln, P.; Nordén, B. DNA-Binding of Semirigid Binuclear Ruthenium Complex $\Delta\Delta$-[μ-(11,11′-bidppz)$(phen)_4Ru_2]^{4+}$: Extremely Slow Intercalation Kinetics. *J. Am. Chem. Soc.* **2002**, *124*, 12092–12093.
39. Frykholm, K.; Morimatsu, K.; Nordén, B. Conserved Conformation of RecA Protein after Executing the DNA Strand-Exchange Reaction. A Site-Specific Linear Dichroism Structure Study. *Biochemistry* **2006**, *45*, 11172–11178.
40. Nordh, J.; Deinum, J.; Nordén, B. Flow Orientation of Brain Microtubules Studied by Linear Dichroism. *Eur. Biophys. J.* **1986**, *14*, 113–122.
41. Brattwall, C. E. B.; Lincoln, P.; Nordén, B. Orientation and Conformation of Cell-Penetrating Peptide Penetratin in Phospholipid Vesicle Membranes Determined by Polarized-Light Spectroscopy. *J. Am. Chem. Soc.* **2003**, *125*, 14214–14215.